SASEC2015
Third Southern African Solar Energy Conference
11 – 13 May 2015
Kruger National Park, South Africa

A One Dimensional Thermal Model for Evacuated Tubes-Based Solar Collectors

Paradis P.L., Rousse D. R.*, and Hallé, S.
*Author for correspondence
t3e Industrial Research Chair,
Département de génie mécanique,
École de technologie supérieure,
1100, rue Notre-Dame O, Montréal (Qc), H3K 1C3
Canada,
E-mail: daniel@t3e.info

ABSTRACT

This paper presents a one dimensional thermal model for an evacuated tube under transient conditions. The first order differential equations derived are solved with a fully explicit scheme using a fourth order Runge-Kutta algorithm. The comparison between simulated and experimentally measured outlet air temperature showed a good agreement as a root mean square error on the outlet air temperature of about 0.52 °C and a mean bias difference of 0.20 °C were observed on a bright sunny day. Finally, the validated model applied for steady state heat transfer is used to conduct an analysis on different parameters. The airflow rate is the most important parameter acting on the defined performance indicators. Higher is the airflow, better is the efficiency and lower is the outlet air temperature. On the other side, a low airflow can lead to as much as 100 °C of temperature gain, but the efficiency is then reduced to values as low as 45 %.

NOMENCLATURE

A	[m^2]	Projected surface
D	[m]	Tube diameter
d	[m]	Glass tube thickness
L	[m]	Tube length
m	[kg]	Mass
c_p	[J/KgK]	Specific heat
n	[-]	Number of node
$\dot{V}$	[m^3/s]	Volumetric airflow
u	[m/s]	Air velocity
$\dot{m}$	[kg/s]	Mass airflow fate
G_T	[W/m^2]	Total tilted solar radiation in the plane of the collector
G	[W/m^2]	Total horizontal solar radiation
G_r	[W/m^2]	Reflected solar radiation
R	[K/W]	Thermal résistance
T	[°C]	Temperature
j	[-]	Indicate the node
i	[-]	Indicate the time step
P	[Pa]	Pressure
Re		Reynolds number
Nu		Nusselt number
$\dot{Q}$	[W]	Thermal power transferred to the fluid

Special characters

τ	[-]	Transmissivity of the glass
α	[-]	Absorptivity of the absorber
ρ	[kg/m^3]	Density
ε	[-]	Emissivity
η	[%]	Efficiency

Subscripts

g	glass
r	receiver tube / absorber tube (outer tube)
c	cover tube (inner tube)
f	fluid (air)
a	Ambient
in	Inner tube
out	Outer tube
conv	Convection heat transfer
ray	Radiative heat transfer
dyn	Dynamic pressure
useful	Useful
inlet	Tube inlet
outlet	Tube outlet

INTRODUCTION

In Canada, more than 50 % of the energy consumption in residential, institutional and commercial sectors is related to space heating and domestic hot water [1]. This heat could be produced with solar thermal collectors with a high level of efficiency.

To avoid glycol and prevent freezing or boiling, air could be used as the heat transfer fluid instead of water. The heat capacity of air is low compared to that of liquids but

nevertheless it is worth trying to design an air-based collector for specific applications despite this drawback. Moreover, as insulation is closely linked to solar collector performance use of solar evacuated tube then makes sense in cold climates to reduce heat losses in winter when the heating demand is highest.

Hence, a new kind of solar evacuated tube collector using air as the working fluid is currently developed by Technology of Energy and Energy Efficiency Research Chair (t3e) of École de technologie supérieure (ETS) in Montréal, Canada. The design involves tubes that are open at both ends thus allowing "through flow" of fluid from one end to the other.

Solar evacuated tubes thermal collector using air as the working fluid has been used for the first time at the end of the 70's. After the oil crisis of 1973, solar thermal was considered part of the solution [2-3]. In this type of collector, outside air is admitted in a cold manifold. Air then goes down heating in contact with the inner wall of the tubes then goes up in an aluminium collector tube. Finally, air flows in a second evacuated tube and reaches the hot manifold. This collector geometry was first analysed by Eberlein [4]. He developed a one dimensional model to analyse the performances of the collector. The one dimensional approach is also used on similar geometries [5-8]. Kumar, et al. [6] and Bansal and Sharma [7] worked on four types of solar tubes, respectively, with and without vacuum and with and without selective absorber coating in order to determine the influence of vacuum and coating on the performances. Kim, et al. [5] present a collector tube filled with a water/glycol mixture used as a liquid film to transfer the heat from the receiver to a first aluminium tube into which flows the working fluid flowing upward.

Although work have previously been done to evaluate and optimise the performance of evacuated tubes [5-8], only few published papers [9, 10] have been found on newly commercialised solar evacuated tubes open at both ends and available on the Chinese market. The purpose of this work is then to propose a yet simple but validated model to qualify the heat exchanges occurring in this kind of tube without traditional costly multidimensional CFD simulations.

THERMAL MODEL

First, a steady state model of the tube in stagnation (without flow) was developed. The equilibrium temperatures (for the inner and outer glass walls called receiver, *r*, and cover, *c*, in the remainder of this work) were obtained from a balance between net gain by radiation and combined convective and radiative losses. This first model involved a simple thermal resistance network for the whole tube. The model was tested against experimental results. It is worth mentioning that for very high radiative fluxes, the temperature of the receiver reached temperatures above 100 °C and one of the tubes exploded due to the high thermal stresses induced by the temperature difference between the cover and receiver welded together.

Then, the model has been modified to take into account unsteady conditions of solar radiation, wind speed and outside air temperature [11]. This problem readily became more involving as the resistance network representation was no longer valid. Nevertheless, the equations were retained and new resistances were calculated from one time step to the next to account for variations with time until convergence. An explicit scheme was implemented. No updates of coefficients (thermal resistances) were required within a given time step. In the third step, a model involving steady-state conditions with fluid flow was elaborated. Hence, as the fluid gained energy, its temperature was increasing along the axis and energy balances were introduced for n discrete slices of the tube. Finally, in order to validate the model in real environmental conditions, the model has been extended for unsteady conditions of mass flow rate, solar radiation, wind speed and outside ambient temperature.

In each of those models, the heat transfer is considered one-dimensional along the radial coordinate and axisymmetric. That is there is only one temperature which characterises the inner and outer glass walls, respectively: for a given axial position, heat is equally distributed azimuthally on the receiver and the cover. Moreover, the conduction resistances in the glass walls are considered negligible: there is only one temperature that characterizes the inner and outer surface and the temperature varies axially essentially because of the heat gained by the fluid. As the walls are thin this makes conduction essentially negligible. All data for variable thermal properties with air temperature are readily available to account for such variations [12].

Figure 1 (a) gives a schematic representation and the control volume used along the longitudinal axis of the tube (left). Furthermore, a representation using the thermal/electrical analogy is used (Figure 1b) to show the radial heat transfer phenomena taking place for a given slice j of the tube.

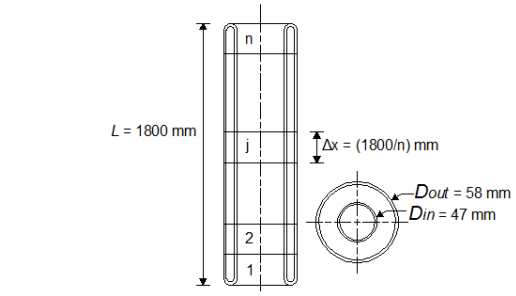

(a)

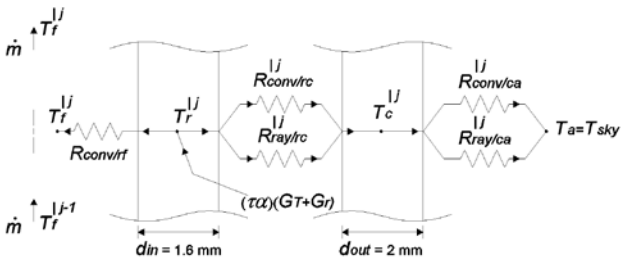

(b)

Figure 1 (a) Schematic of the vacuum tube and (b)Thermal model

With respect to the above-mentioned assumptions a unique temperature is used to define the cover temperature (outer glass tube wall) T_c, and the receiver temperature (inner glass tube wall) T_r. Finally, T_f is the mean temperature of the fluid for a given node *j*.

To solve for the three unknowns (T_c, T_r and T_f), three independent equations are written for each control volume of the tube along the longitudinal coordinate. According to the first law of thermodynamic and from Figure 1, we have for the fluid involved in c.v. *j*:

$$\underbrace{\left(\frac{m_f c_{p/f}^{|j}}{n}\right)\frac{dT_f^{|j}}{dt}}_{\text{Energy stored in the c.v.}} = \underbrace{\rho_f^{|j-1}\dot{V}_f c_{p/f}^{|j-1} T_f^{|j-1}}_{\text{Energy entering the c.v.from the previous node}} + \underbrace{\left[\frac{1}{R_{conv/rf}^{|j}}\right]\left(T_r^{|j} - T_f^{|j}\right)}_{\text{Energy leaving the c.v. in convective heat transfer from the receiver to the fluid}} - \underbrace{\rho_f^{|j}\dot{V}_f c_{p/f}^{|j} T_f^{|j}}_{\text{Energy leaving the c.v. to the next node}} \quad (1)$$

The convective heat transfer coefficient is obtained by use of three different correlations according to the flow regime (laminar, transition or turbulent) provided in standard textbooks such as that of Incropera, et al. [16]. The Nusselt number for a constant heat flux at the boundary is used for Reynolds number below 2300, then the Gnielinski correlation is employed for $3000 < Re < 10\,000$ while the Dittus Boelter correlation is used for $Re > 10\,000$. The transition between each correlation is smoothed with a linear interpolation to cover the full range of the Reynolds numbers involved.

For the receiver (the inner glass wall involving the absorption coating) in slice j:

$$\underbrace{\left(\frac{m_{g/in} c_{p/g}}{n}\right)\frac{dT_r^{|j}}{dt}}_{\text{Energy stored in the c.v.}} = \underbrace{(\tau_c\alpha_r)(G_T + G_r) D_{in}\frac{L}{n}}_{\text{Energy entering the c.v. from solar radiation}} - \underbrace{\left[\frac{R_{conv/rc}^{|j} + R_{ray/rc}^{|j}}{R_{conv/rc}^{|j} R_{ray/rc}^{|j}}\right]\left(T_r^{|j} - T_c^{|j}\right)}_{\text{Energy leaving the c.v. in convective and radiative heat transfer from the receiver tube to the cover tube}} - \underbrace{\left[\frac{1}{R_{conv/rf}^{|j}}\right]\left(T_r^{|j} - T_f^{|j}\right)}_{\text{Energy leaving the c.v. in convective heat transfer to the fluid}} \quad (2)$$

In Eq.2, "$(\tau\alpha)$" is the standard effective absorptivity-transmissivity couple provided by Duffie and Beckman [17]. The thermal resistances are again found in Incropera et al. [16]. "$R_{conv/rc}$" is the convection resistance between the receiver and the cover (in the vacuum annular space). In the original work proposed by Eberlein in 1976, this resistance was completely neglected assuming perfect vacuum. Here, the assumption of continuous medium does not hold and using an "effective convective heat transfer coefficient" in a partial vacuum may be hazardous. Nevertheless, several values of effective heat transfer coefficient were used without significant changes into solutions. "$R_{ray/rc}$" is the radiative resistance between the receiver and the cover. The long infinite cylinder approximation [16] is used to evaluate this resistance although the tube is discretized into small slices along the longitudinal axis (view factors – and hence radiative coupling – between slices is not considered).

Finally, for the cover in slice j:

$$\underbrace{\left(\frac{m_{g/out} c_{p/g}}{n}\right)\frac{dT_c^{|j}}{dt}}_{\text{Energy stored in the c.v.}} = \underbrace{\left[\frac{R_{conv/rc}^{|j} + R_{ray/rc}^{|j}}{R_{conv/rc}^{|j} R_{ray/rc}^{|j}}\right]\left(T_r^{|j} - T_c^{|j}\right)}_{\text{Energy entering the c.v. in convective and radiative heat transfer from the receiver tube to the cover tube}} - \underbrace{\left[\frac{R_{conv/ca}^{|j} + R_{ray/ca}^{|j}}{R_{conv/ca}^{|j} R_{ray/ca}^{|j}}\right]\left(T_c^{|j} - T_a\right)}_{\text{Energy leaving the c.v. in convective and radiative heat transfer from the cover tube to the ambient}} \quad (3)$$

The correlation proposed by Zukauskas for a single tube in a cross flow is implemented to evaluate the convection coefficient with the wind speed supposed perpendicular to the tube. Finally, "$R_{ray/ca}$" is the radiative resistance between the cover and the environment. The approximation of a small object in a large environment of uniform temperature is used. Furthermore, the surrounding radiative temperature is set equal to the ambient temperature as a simplification. Strictly, this should underestimate heat losses for bright and clear days as the effective "sky" temperature T_{sky} would be lower than T_a.

To complete this model, the glass properties are assumed to be constant while the fluid (air) properties inside the tubes and in the environment are function of the temperature. Table 1 shows a brief summary of the parameters used in the model.

Table 1 Numerical value of the parameters used in the model

Parameter	Value	Units
D_{out}	0.058	m
D_{in}	0.047	m
d_{out}	0.002	m
d_{in}	0.0016	m
α_r	95	%
τ_c	95	%
ε_τ	4 $0.022T_r$ - 2.37 [18]	% for $0\ K \le T_r \le 293\ K$ % for $293\ K \le T_r \le \infty$
ε_c	90	%
L	1.8	m
ρ_g	2230	kg/m^3
$c_{p/g}$	837.2	J/kg K
air properties	function of T_f	using Incropera, et al. [16] data

Using the environmental parameters (solar radiation, wind speed, ambient temperature) and the operating parameter (airflow) as input parameters for the model, it's possible to simulate the outlet air temperature in transient conditions. A fourth order Runge-Kutta method is used to solve the time derivatives. Figure 2 shows the resolution algorithm implemented in Matlab.

VALIDATION

Figure 3 presents a comparison of experimental results and predictions for a bright sunny day. The measurements are

carried out around solar noon to reduce the sensibility of the measurement made with a fixed pyranometer in the plane of the collector [13]. The complete description of the experimental set-up can be consulted in [14].

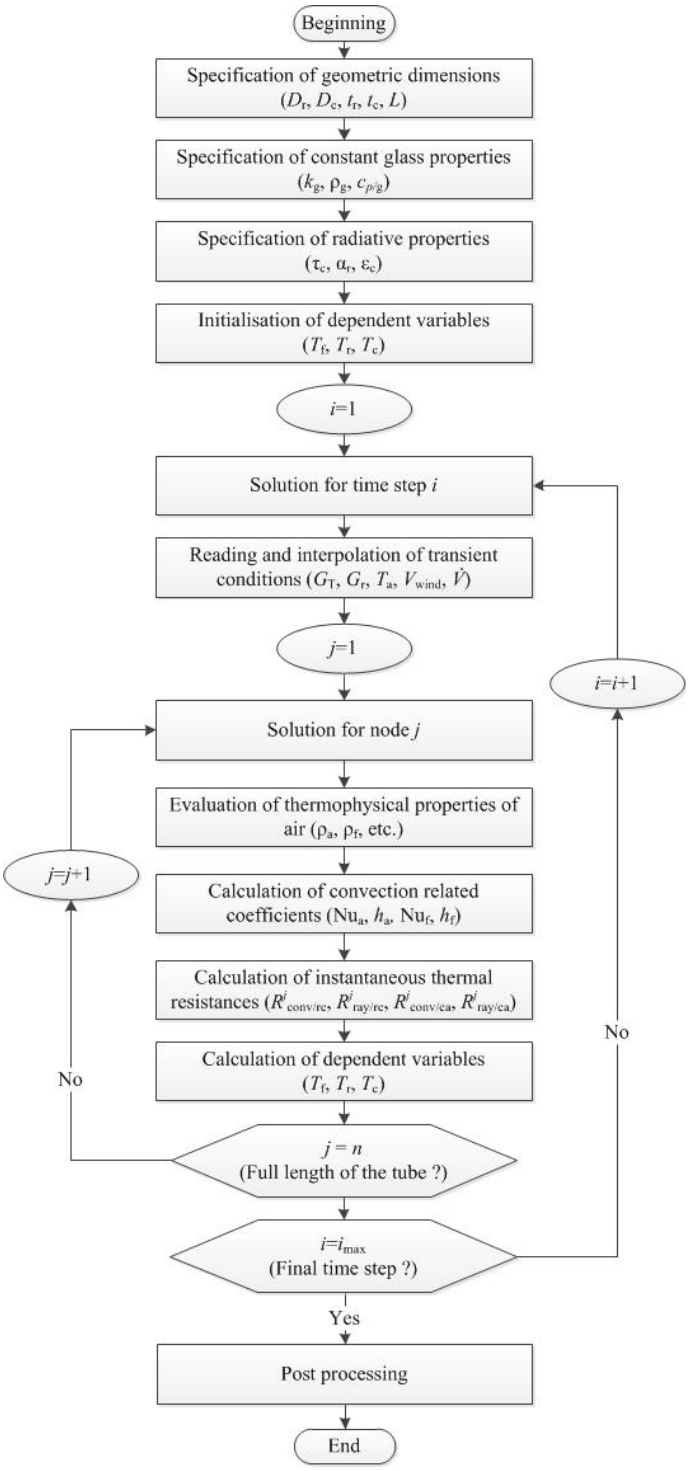

Figure 2 Resolution algorithm implemented in Matlab

The simulation presented in Figure 3 involved results obtained with only 3 nodes which provide a good compromise between the precision of the solution and calculation time. A time step of 0.01 second was used to respect the CFL criterion. Results for several days were compared to assess the validity of the predictions over a period of four months.

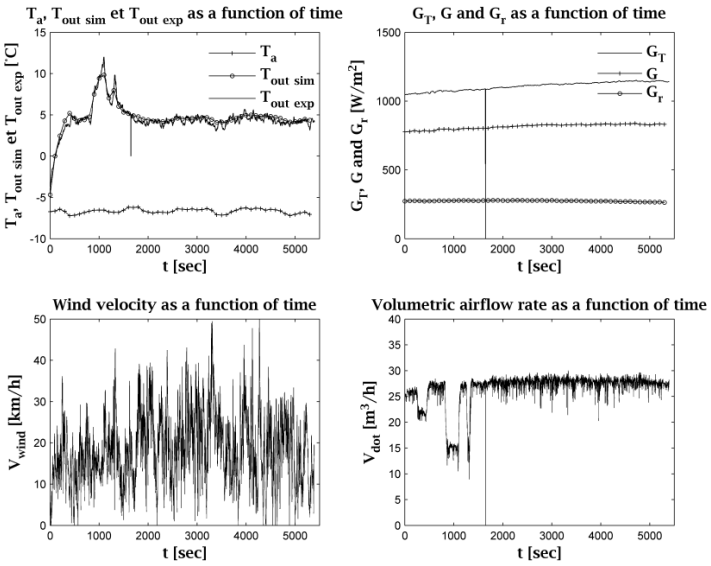

Figure 3 Validation of the model with experimental results

Figure 3 presents four graphs, the upper left one shows the outlet air temperature (experimental data and simulated one) and the ambient temperature. On the upper right graph the three measured solar radiations are shown. G_T is measured in the plane of the tube, G is the total horizontal solar radiation and G_r is the reflected solar radiation. G is not used explicitly as an input for the simulation model, but the information was available from the weather station and is given here as a piece of additional information. The wind speed is presented on the third lower left graph. Finally, the volumetric airflow rate is shown on the last graph (lower right corner). The mean value is around 30 m^3/h and variations have been manually induced to test the transient behavior of the model (the flow was reduced to about 15 m^3/h). Some noise is present on the airflow rate measurement. This noise is due to the wind. In fact, as the dynamic pressure is measured to obtain the airflow rate indirectly, and the end of the tube is open to ambient air, the wind necessarily influences this measurement. All graphs involve a reading error at about 1700 s where the system sent back a 0 value.

The upper left graph in Figure 3 shows that although the model doesn't exhibit the rapid variations of temperature (probably caused by the turbulence of the flow), the numerical model (line with circles) follows very well the experimental (continuous line) behavior of the tube. A root mean square error of 0.52 °C and a mean bias difference of 0.20 °C are then obtained. Since the gain in temperature is around 10 °C a difference of 0.52 °C is in the range of the precision of the type T thermocouple but in general the model overestimates the outlet temperature of 0.20 °C. Moreover, this could be explained by the assumption that $T_a = T_{sky}$ in the model which

slightly reduces the heat losses to the environment. Finally, the precision of the velocity (pressure) sensors, the experimental uncertainty and the correlations used to determine the convection coefficient may explain the differences.

With a validated model, it is possible to analyse the influence of the environmental conditions (ambient temperature, wind speed, solar radiation) and operation (airflow) parameters on the performances of the tube using this transient model in steady state.

STEADY STATE PREDICTIONS

The preceding model (Eqs.1-3) can be solved in steady state. In this case, the energy storage term becomes 0 and the Runge-Kutta method is no longer needed. In fact, in steady state a simple linear system of equation is obtained that can be solved for the three unknown temperatures at each node *j*. Matlab matrix inversion capabilities are conveniently used to realise this. Initial values of the coefficients are used since these coefficients (the thermal resistances) depend on the final solution (the temperature at each node). Hence, the linear system of equation is solved iteratively. The model is then used to see the impact of different factors used to characterise the performances of the tube: outlet air temperature, T_{out}, mean global heat transfer coefficient (inside the tube), HTC, thermal efficiency, η, and the pressure drop, ΔP. The pressure drop is calculated using the Colebrook correlations [15]. The thermal efficiency is defined according to the following equation:

$$\eta = \frac{\dot{Q}_{\text{useful}}}{G_T A} \times 100\% \tag{4}$$

Where $\dot{Q}_{\text{useful}}$ is defined as:

$$\dot{Q}_{\text{useful}} = \dot{m}(c_{p/\text{outlet}} T_{\text{outlet}} - c_{p/\text{inlet}} T_{\text{inlet}}) \tag{5}$$

Eq.5 is a standard expression but here the definition of the surface area, *A*, is important to specify. As a single tube is investigated, *A* is based upon the external diameter of the outside tube (cover), D_{out}. Strictly, this would mean that a multi tubes collector would involve no spacing between tubes which is usually not the case. This implies that rather large efficiencies are expected for the single tube.

Figure 4 shows the influence of solar radiation G_T on T_{out}, HTC, η, and ΔP with $T_a = 20$ °C, $V_{wind} = 5$ km/h, and $\dot{V} = 30$ m^3/h. Spatial discretization was performed with 100 nodes located every 1.8 cm along the tube. The mesh independency of the solution has been verified and no significant differences have been identified above 10 nodes.

Figure 4 presents four graphs, the upper left one shows the influence of solar radiation on the outlet temperature. On the upper right graph the heat transfer coefficient as a function of the solar radiation is presented. Influence on efficiency is also presented on the third lower left graph. Finally, the impact on pressure drop is shown on the last graph (lower right corner). All following figures are constructed as such.

These results show a negligible influence of solar radiation on the pressure drop, efficiency and heat transfer coefficient. Pressure drop and HTC variations are simply due to variations in thermophysical properties.

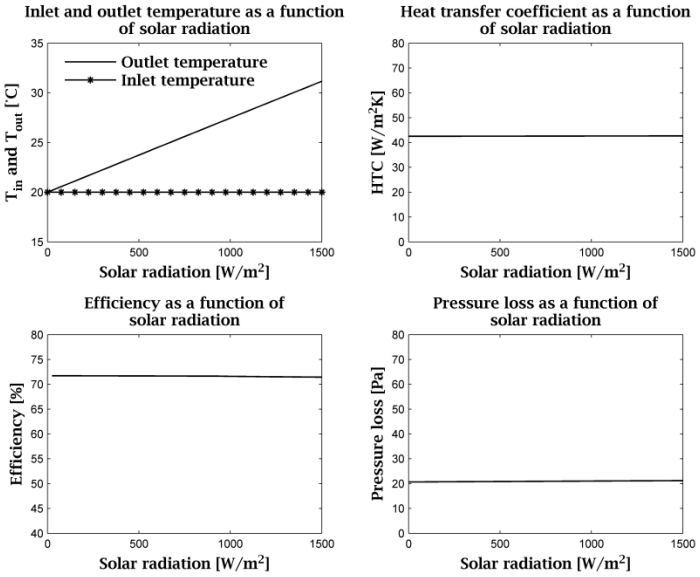

Figure 4 Influence of solar radiation G_T [W/m^2] on T_{out} [°C], HTC [W/m^{2}K], η, and ΔP [Pa] ($T_a = 20$ °C, $V_{wind} = 5$ km/h, and $\dot{V} = 30$ m^3/h)

Efficiency calculations based on the projected surface area of the tube imply that the losses in efficiency are mainly due to the solar radiation reflected by the cover, the losses by the cover by radiation and convection and the geometrical loss due to the fact that the inner tube as a smaller diameter than the outer tube. As the convective losses are nearly constant for the range of temperature variations considered here, the efficiency is nearly constant decreasing about 2% with the increase of G_T. Hence, with a nearly constant η, the temperature increase with G_T is nearly linear as shown in the upper left graph. The outlet temperature is identical to the ambient temperature when there is no solar radiation and the efficiency drops to 0. The outlet air temperature increases almost linearly with the augmentation of solar radiation to attain an augmentation of 11.2 °C over the ambient temperature at 1500 W/m^2 of solar radiation. The more the source term (Eq.2) increases, the more the fluid will absorb energy.

Figure 5 shows the influence of the volumetric airflow rate $\dot{V}$ on T_{out}, HTC, η, and ΔP with $T_a = 20$ °C, $V_{wind} = 5$ km/h, and $G_T = 1000$ W/m^2. 100 nodes were still used. This figure shows the strong influence of the inner volumetric air flow rate on the performances of the tube double-walled tube. The influence of the flow rate is of primary importance in air collector [16]. For small flow rates a temperature gain above 100 °C can be obtained. But in this case, the efficiency is quite low due to higher heat loss of the evacuated tube to the surrounding by radiation and convection. As the airflow rate increases, the temperature gain goes down to almost 0 (above 40 m^3/h) and the efficiency reaches about 70 %. As the thermal losses reduce to almost zero with a high flow rate and constant optical losses (radiative properties are considered independent of *T*), this

explains why the maximum efficiency asymptotically tends to 70 % with low convective losses. Naturally, as the flow rate increases, the pressure drop increases too as it usually varies with the square of the fluid velocity. Finally, there is three different sections for the convective heat transfer coefficient to the heat transfer fluid (one for each flow regime: laminar, transition, turbulent) due to the use of three different correlation (on for each of the flow regime). This explains the somewhat irregular shape of the curve for HTC.

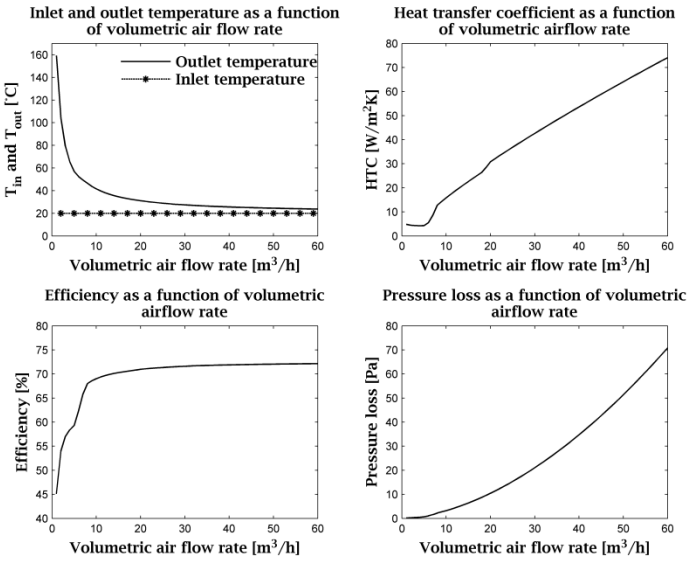

Figure 5 Influence of the volumetric airflow rate $\dot{V}$ [m3/h] on *T*out [°C], HTC [W/m2K], η, and ΔP [Pa] (*T*a = 20 °C, *V*wind = 5 km/h, and *G*T = 1000 W/m2)

The influence of wind speed and ambient temperature were also investigated but results will be presented at the conference to avoid making this paper overly lengthy.

CONCLUSION

A simple axisymmetric 1D model of the heat exchanges taking place in a single evacuated solar tube is presented and experimental validation results are provided. A good agreement between the simulations and the experimental measurements is found: a root mean square error of 0.52 °C is calculated on the outlet airflow temperature, T_{out}.

The steady state model is used to explore the impact of the weather and operation parameters on different performance indicators (outlet temperature T_{out} [°C], heat transfer coefficient HTC [W/m^{2}K], efficiency η, and pressure drop ΔP [Pa]). The volumetric airflow rate is shown to be the parameter with the most influence on the performances.

This work is the basis of a program aimed at designing thermal solar collectors using air as the working fluid and evacuated tubes opened at both ends as the basic component. Future work should include the development of tubes that could sustain the constraints caused by the thermal expansion of the hot inner tube (receiver) for very low or no airflow.

ACKNOWLEDGMENT

First author acknowledge the Natural Sciences and Engineering Research Council of Canada (NSERC) for Alexander Graham Bell scholarship and Fonds de recherche du Québec – Nature et technologies and Ecosystem for support. The authors also thank the partners of the t3e research chair who support the project.

REFERENCES

[1] Ressources naturelles Canada, Energy Efficiency Trends in Canada 1990 to 2009, in, 2011.
[2] K. L. Moan, Tubular solar energy collection system utilizing air media, in, L. Moan, Kenneth, État-Unis, 1976.
[3] H.E. Novinger, Low profile evacuated-bottle solar collector module, in, Novinger, Harry E., État-Unis, 1980.
[4] M.B. Eberlein, Analysis and Performance Predictions of Evacuated Tubular Solar Collectors Using Air as the Working Fluid, University of Wisconsin, 1976.
[5] J.T. Kim, H.T. Ahn, H. Han, H.T. Kim, W. Chun, The performance simulation of all-glass vacuum tubes with coaxial fluid conduit, International Communications in Heat and Mass Transfer, 34 (2007) 587-597.
[6] R. Kumar, S.C. Kaushik, H.P. Garg, Transient analysis of evacuated tubular solar collector with finite difference technique, Renewable Energy, 4 (1994) 941-947.
[7] N. Bansal, A. Sharma, Transit theory of a tubular solar energy collector, Solar energy, 32 (1984) 67-74.
[8] H. Liang, Experimental research on the all-glass evacuated tube solar air collector, in: D.Y. Goswami, Y. Zhao (Eds.) Proceedings of ISES World Congress 2007 (Vol. I – Vol. V), Springer Berlin Heidelberg, 2009, pp. 674-677.
[9] L.J. Shah, S. Furbo, Vertical evacuated tubular-collectors utilizing solar radiation from all directions, Applied Energy, 78 (2004) 371-395.
[10] L.J. Shah, S. Furbo, Modeling shadows on evacuated tubular collectors with cylindrical absorbers, TRANSACTIONS-AMERICAN SOCIETY OF MECHANICAL ENGINEERS JOURNAL OF SOLAR ENERGY ENGINEERING, 127 (2005) 333.
[11] P.-L. Paradis, S. Hallé, G. Quesada Ramos, D. R. Rousse, L. Guillon, Modèle thermique d'un tube sous vide en stagnation, in: AMT 2014, Agadir, Maroc, 2014.
[12] F.P. Incropera, A.S. Lavine, D.P. DeWitt, Fundamentals of heat and mass transfer, John Wiley & Sons Incorporated, 2011.
[13] J.A. Duffie, W.A. Beckman, Solar engineering of thermal processes, John Wiley & Sons, Inc., New Jersey, 2006.
[14] P.L. Paradis, D.R. Rousse, S. Hallé, L. Lamarche, G.Quesada, Thermal modeling of evacuated tubes-solar air collectors, (Submitted to Solar Energy, July 2014).
[15] F.M. White, Fluid mechanics, 7 th ed. ed., McGraw-Hill, New York, 2011.
[16] V. Delisle, M. Kummert, Experimental Study to Characterize the Performance of Combined Photovoltaic/Thermal Air Collectors, J. Sol. Energy Eng, 134 (2012).